Catalysis Today 153 (2010) 70–76

Contents lists available at ScienceDirect

Catalysis Today

journal homepage: www.elsevier.com/locate/cattod

Selective catalytic reduction of NO with NH_3 over manganese substituted iron titanate catalyst: Reaction mechanism and H_2O/SO_2 inhibition mechanism study

Fudong Liu, Hong He*

State Key Laboratory of Environmental Chemistry and Ecotoxicology, Research Center for Eco-Environmental Sciences, Chinese Academy of Sciences, Beijing 100085, PR China

ARTICLE INFO

Article history:
Available online 24 March 2010

Keywords:
Selective catalytic reduction
Iron titanate catalyst
Mn substitution
SCR mechanism
Ammonium nitrate
H_2O/SO_2 inhibition effect

ABSTRACT

Selective catalytic reduction (SCR) of NO with NH_3 over Mn substituted iron titanate catalyst ($Fe_{0.75}Mn_{0.25}TiO_x$) was fully investigated using *in situ* diffuse reflectance infrared Fourier transform spectroscopy. At relatively low temperatures, both ionic NH_4^+ and coordinated NH_3 contributed to the SCR reaction, and both bridging nitrate and monodentate nitrate were confirmed to be the reactive nitrate species. In the SCR reaction condition, surface NH_4NO_3 species was formed as intermediate species and its reactivity was also proved. An NH_3-SCR mechanism over $Fe_{0.75}Mn_{0.25}TiO_x$ at low temperatures was proposed accordingly, in which the reduction of NH_4NO_3 by NO was possibly the rate-determining step. Due to the mild and reversible inhibition effect of H_2O on NH_3/NO_x adsorption, the SCR activity decline in the presence of H_2O was also slight and recoverable; however, the inhibition effect of SO_2 was much more intense and irreversible, because the formation of nitrate species was totally inhibited by the formation of sulfate, resulting in the cut-off of the SCR reaction pathway at low temperatures.

© 2010 Elsevier B.V. All rights reserved.

1. Introduction

Selective catalytic reduction (SCR) of NO with NH_3 is a well-proven technique for the removal of NO_x in exhaust gases from stationary and mobile sources, and the most widely used commercial catalyst system is V_2O_5–WO_3 (MoO_3)/TiO_2 [1], of which the operation temperature window is usually at 350–400 °C. Such a catalyst system cannot be used in the NO_x removal process for the flue gas after dust removal and desulfurization from coal-fired power plants or the exhaust gas from diesel engines in cold-start process due to the low exhaust temperature (< 200 °C). Therefore, many researchers are devoted to the development of low temperature SCR catalysts, such as V_2O_5 loaded on AC (activated carbon)/Al_2O_3/carbon–ceramic [2–4], Fe–Mn oxides loaded on TiO_2/USY zeolite/mesoporous silica [5–7], pure MnO_x [8–10], MnO_x loaded on TiO_2/Al_2O_3/SiO_2/AC/USY zeolite [6,11–13], and Mn–Cu, Mn–Ce mixed oxides [14–16].

In our previous study, we have also developed a novel iron titanate catalyst ($FeTiO_x$) showing high SCR activity, N_2 selectivity and H_2O/SO_2 durability in the medium temperature range (200–400 °C) [17,18]. In the relatively low and high temperature ranges, Langmuir–Hinshelwood mechanism and Eley–Rideal mechanism mainly dominated in the NH_3-SCR reaction, respectively [19]. Through the substitution of partial Fe by Mn, the low temperature SCR activity was greatly enhanced with more than 90% NO_x conversion obtained from 150 to 325 °C; the influence of Mn substitution on the structure and activity of iron titanate catalyst was also fully investigated [20]. In this paper, the SCR reaction mechanism over $Fe_{0.75}Mn_{0.25}TiO_x$ catalyst at low temperatures will be studied using *in situ* diffuse reflectance infrared Fourier transform spectroscopy (*in situ* DRIFTS). The inhibition effect of H_2O and SO_2 will also be clarified, which is important to the further improvement of the SCR performance and H_2O/SO_2 resistance for its practical application.

2. Experimental

2.1. Catalyst synthesis and activity test

$Fe_{0.75}Mn_{0.25}TiO_x$ catalyst was prepared by conventional co-precipitation method using $Fe(NO_3)_3{\cdot}9H_2O$, $Mn(NO_3)_2$ and $Ti(SO_4)_2$ as precursors. The detailed synthesis process was described in our previous study [20]. The influence of H_2O/SO_2 on the NO_x conversion in the NH_3-SCR reaction over $Fe_{0.75}Mn_{0.25}TiO_x$ catalyst was conducted in a fixed-bed quartz tube reactor at atmospheric pressure. The reaction conditions were controlled as follows: 500 ppm NO, 500 ppm NH_3, 5 vol.% O_2, 10 vol.% H_2O

* Corresponding author at: P.O. Box 2871, 18 Shuangqing Road, Haidian District, Beijing 100085, PR China. Tel.: +86 10 62849123; fax: +86 10 62849123.
E-mail address: honghe@rcees.ac.cn (H. He).

0920-5861/$ – see front matter © 2010 Elsevier B.V. All rights reserved.
doi:10.1016/j.cattod.2010.02.043

(when used), 100 ppm SO_2 (when used), N_2 balance; 0.6 ml catalyst, total flow rate of 500 ml/min and gas hourly space velocity (GHSV) = 50 000 h^{-1}. The effluent gas was analyzed using an FTIR spectrometer (Nicolet Nexus 670) equipped with a heated, low volume multiple-path gas cell (2 m).

2.2. Mechanism study

The *in situ* DRIFTS experiments were performed on an FTIR spectrometer (Nicolet Nexus 670) equipped with an MCT/A detector cooled by liquid nitrogen and an *in situ* DRIFTS reactor cell with ZnSe window (Nexus Smart Collector) connected to a purging/adsorption gas control system. The reaction temperature was controlled precisely by an Omega programmable temperature controller. Prior to each experiment, the sample was pretreated at 400 °C in a flow of 20 vol.% O_2/N_2 for 0.5 h and then cooled down to the desired temperature. The background spectrum was collected in flowing N_2 atmosphere and was automatically subtracted from the sample spectrum. The total flow rate of the feeding gas was kept at 300 ml/min, and all spectra were recorded by accumulating 100 scans with a resolution of 4 cm^{-1}. The reaction conditions were controlled as follows: 500 ppm NO, 500 ppm NH_3, 5 vol.% O_2, 1 vol.% H_2O (when used), 100 ppm SO_2 (when used) and N_2 balance.

3. Results and discussion

3.1. NH_3-SCR mechanism over Mn substituted iron titanate catalyst

3.1.1. In situ DRIFTS of the reaction between NO + O_2 and adsorbed NH_3 species

Fig. 1 shows the *in situ* DRIFTS spectra of the reaction between NO + O_2 and pre-adsorbed NH_3 species on the $Fe_{0.75}Mn_{0.25}TiO_x$ catalyst at 150 °C. After NH_3 pre-adsorption and N_2 purge, the catalyst surface was mainly covered by ionic NH_4^+ (δ_s at 1676 cm^{-1} and δ_{as} at 1443 cm^{-1}) bound to Brønsted acid sites and coordinated NH_3 (δ_{as} at 1603 cm^{-1} and δ_s at 1180 cm^{-1}) bound to Lewis acid sites [21–23]. N–H stretching vibration modes at 3361, 3255 and 3155 cm^{-1} also showed up, together with the negative bands at 3703 and 3362 cm^{-1} due to the hydroxyl consumption through interaction with NH_3 to form NH_4^+. The negative band at 1358 cm^{-1} was mainly caused by the coverage of residual sulfate species ($\nu_{asS=O}$) [23] from the $Ti(SO_4)_2$ precursor, indicating again the existence of Brønsted acid sites on the catalyst surface. After

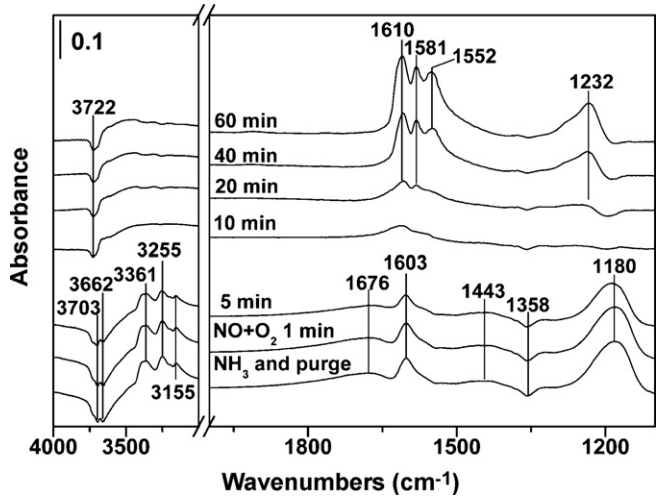

Fig. 1. *In situ* DRIFTS of the reaction between NO + O_2 and pre-adsorbed NH_3 species on the $Fe_{0.75}Mn_{0.25}TiO_x$ catalyst at 150 °C.

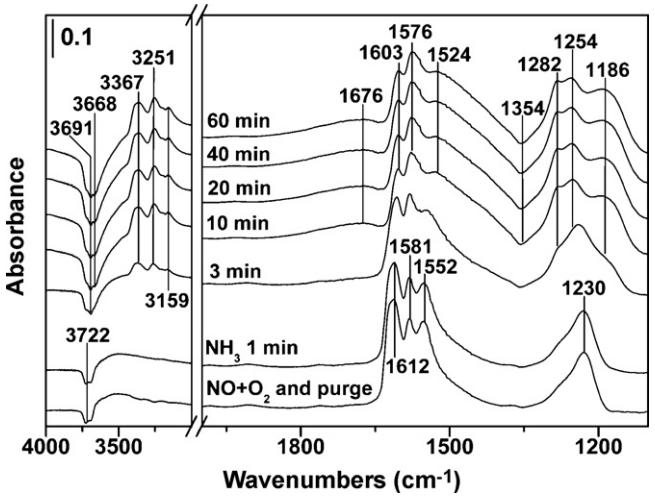

Fig. 2. *In situ* DRIFTS of the reaction between NH_3 and pre-adsorbed NO_x species on the $Fe_{0.75}Mn_{0.25}TiO_x$ catalyst at 150 °C.

the introduction of NO + O_2, both the bands attributed to ionic NH_4^+ and coordinated NH_3 showed an obvious decrease in intensity, and totally disappeared after 10 min. This result implied that both ionic NH_4^+ and coordinated NH_3 could play the roles as reducing agents to reduce NO_x in the SCR reaction. Only after the pre-adsorbed NH_3 species was completely consumed, the nitrate species began to accumulate on the catalyst surface, including bridging nitrate at 1610 cm^{-1} (ν_3 high) and 1232 cm^{-1} (ν_3 low), bidentate nitrate at 1581 cm^{-1} (ν_3 high) and monodentate nitrate at 1552 cm^{-1} (ν_3 high) [24,25]. Besides, the *in situ* DRIFTS spectra in Fig. S1 (Supporting Information) showed that the nitrate species could not form after the introduction of NO + O_2 if NH_3 was supplied successively in the simulating gas, indicating that the consumption of active nitrate species was very fast during this process.

3.1.2. In situ DRIFTS of the reaction between NH_3 and adsorbed NO_x species

Contrastively, we performed another *in situ* DRIFTS experiment of the reaction between NH_3 and pre-adsorbed NO_x species on the $Fe_{0.75}Mn_{0.25}TiO_x$ catalyst at 150 °C, of which the results are shown in Fig. 2. As we have known, after the pre-adsorption of NO + O_2 and N_2 purge, the catalyst surface was mainly covered by three kinds of nitrate species. The subsequent introduction of NH_3 resulted in the rapid disappearance of bridging nitrate (1612 and 1230 cm^{-1}) and monodentate nitrate (1552 cm^{-1}), implying that these two kinds of nitrate species were reducible or reactive in the SCR reaction. Oppositely, the bidentate nitrate species (1581 or 1576 cm^{-1}) always existed on the catalyst surface even after 60 min, showing that this species was inactive in the SCR reaction once formed. Similar phenomenon was also observed over our iron titanate catalyst [19] and MnO_x/Al_2O_3 catalyst by other researchers at relatively low temperatures [26]. Simultaneously, adsorbed NH_3 species rapidly occurred on the catalyst surface, *i.e.* ionic NH_4^+ at 1676 cm^{-1} and coordinated NH_3 at 1603 and 1186 cm^{-1}. During this process, additional bands locating at 1524, 1282 and 1254 cm^{-1} showed up, belonging to neither NH_3 nor NO_x species separately. Similar bands also showed up after the introduction of NH_3 when NO + O_2 was supplied successively in the simulating gas (Fig. S2 in Supporting Information).

We assumed that this species was surface ammonium nitrate (NH_4NO_3), originating from NO_2 dimerization, disproportion in the presence of trace of H_2O (producing HONO and HNO_3) and successive reaction with NH_3 [27–29]. In this process, the produced ammonium nitrite (NH_4NO_2) was easy to decompose even at very low temperatures, giving out N_2 and H_2O; however, NH_4NO_3

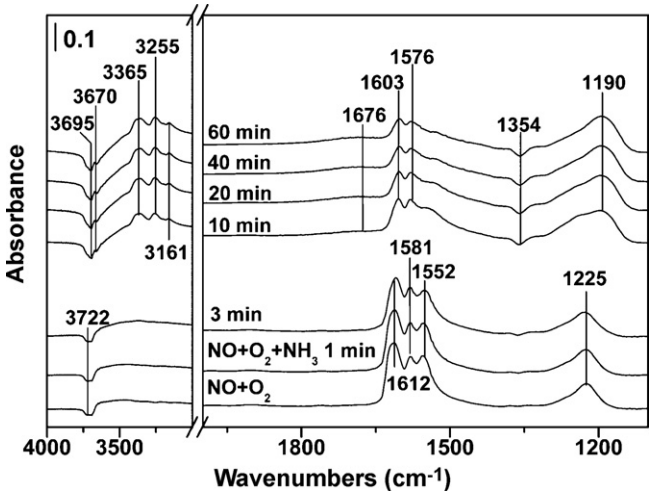

Fig. 3. *In situ* DRIFTS of the reaction on the $Fe_{0.75}Mn_{0.25}TiO_x$ catalyst at 200 °C, during which NO + O_2 was let in firstly and NH_3 was let in subsequently.

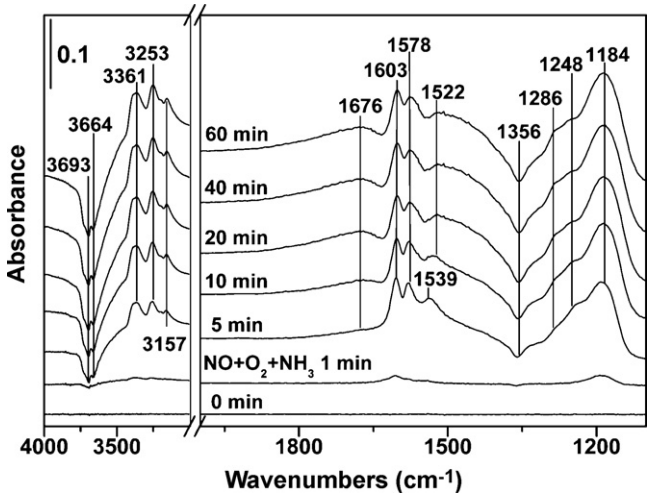

Fig. 5. *In situ* DRIFTS of the NH_3-SCR reaction on the $Fe_{0.75}Mn_{0.25}TiO_x$ catalyst at 150 °C.

could exist on the catalyst surface stably, because its decomposing temperature is *ca.* 200 °C [27]. Therefore, we performed another experiment at 200 °C to see whether this surface species could form on the catalyst surface, during which NH_3 was subsequently introduced with the successive supply of NO + O_2. As shown in Fig. 3, this species was indeed absent at 200 °C, suggesting the possible validity of our previous assumption.

3.1.3. Confirmation of the formation of NH_4NO_3 species

To further confirm the formation of NH_4NO_3 species, we performed another *in situ* DRIFTS experiment of NH_3 adsorption at 150 °C on the $Fe_{0.75}Mn_{0.25}TiO_x$ catalyst pre-impregnated with HNO_3, during which NH_4NO_3 could form directly on the catalyst surface. As the results shown in Fig. 4, besides of the band at 1425 cm^{-1} ascribed to ionic NH_4^+ and negative bands at 1623, 1595 and 1556 cm^{-1} ascribed to the reduction or coverage of nitrate species by NH_3, the bands at 1524, 1286 and 1257 cm^{-1} showed an obvious increase in intensity with the increasing of adsorption time. These bands were located at the same positions as those in Fig. 2 (*i.e.* 1524, 1282 and 1254 cm^{-1}), further proving that the additional bands appeared in Figs. 2 and S2 were indeed due to the formation of adsorbed NH_4NO_3 species.

3.1.4. In situ DRIFTS of the SCR reaction

To investigate the surface species in the real SCR reaction condition, the *in situ* DRIFTS spectra were recorded in a flow of NO + O_2 + NH_3 on the $Fe_{0.75}Mn_{0.25}TiO_x$ catalyst at 150 °C. As the results shown in Fig. 5, the bands attributed to ionic NH_4^+ (1676 cm^{-1}), coordinated NH_3 (1603 and 1184 cm^{-1}) and bidentate nitrate (1578 cm^{-1}) showed up with the increasing of reaction time. Besides, the bands at 1522, 1286 and 1248 cm^{-1} also appeared, similar as those in Figs. 2 and S2, suggesting that the surface NH_4NO_3 might be an important intermediate species in the real SCR reaction. In the following section, the reactivity of NH_4NO_3 species in the SCR reaction will be clarified.

3.1.5. Reactivity of in situ-formed and pre-impregnated NH_4NO_3 on $Fe_{0.75}Mn_{0.25}TiO_x$

The *in situ* DRIFTS experiment of reaction at 150 °C between NO + O_2 and *in situ*-formed NH_4NO_3 species on the $Fe_{0.75}Mn_{0.25}TiO_x$ catalyst was firstly conducted. As the results shown in Fig. 6, after 60 min reaction in a flow of NO + O_2 + NH_3, the surface NH_4NO_3 species was *in situ*-formed with the IR bands at 1522, 1286 and 1252 cm^{-1}. Then, the NH_3 supply was cut off from the simulating gas, making NO + O_2 to react with the surface species. With the increasing of reaction time, not only the bands attributed

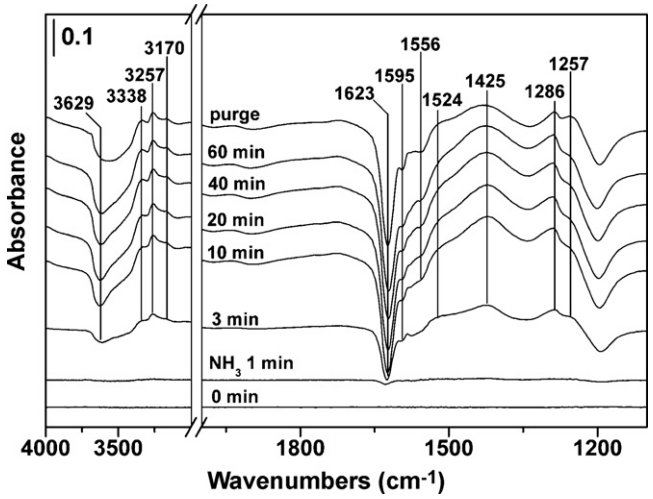

Fig. 4. *In situ* DRIFTS of NH_3 adsorption at 150 °C on the $Fe_{0.75}Mn_{0.25}TiO_x$ catalyst pre-impregnated with HNO_3.

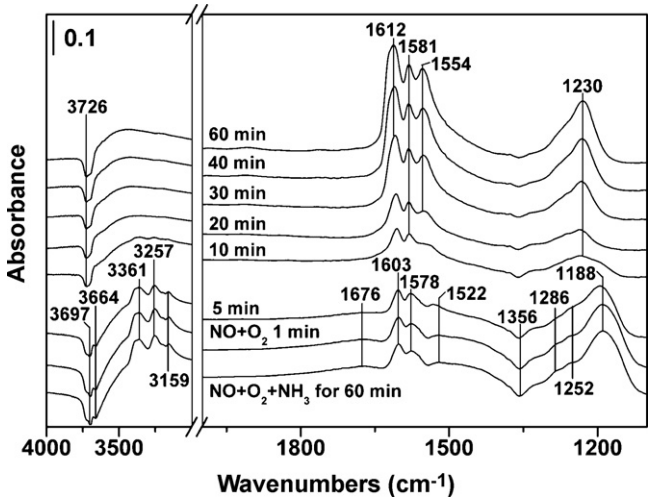

Fig. 6. *In situ* DRIFTS of the reaction between NO + O_2 and *in situ*-formed NH_4NO_3 on the $Fe_{0.75}Mn_{0.25}TiO_x$ catalyst at 150 °C.

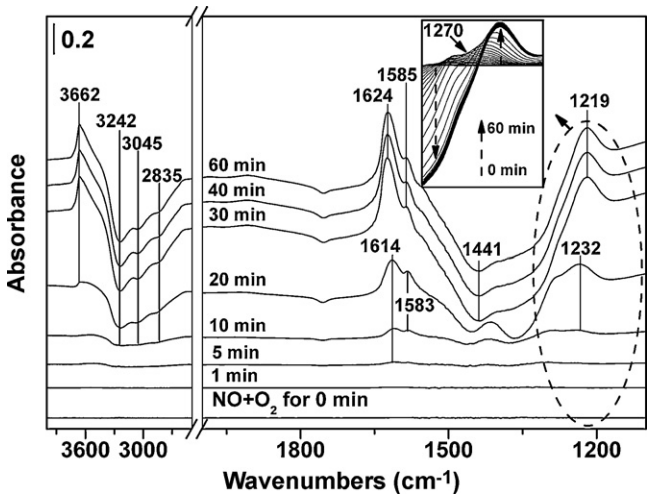

Fig. 7. *In situ* DRIFTS of the reaction between NO + O_2 and pre-impregnated NH_4NO_3 on the $Fe_{0.75}Mn_{0.25}TiO_x$ catalyst at 150 °C.

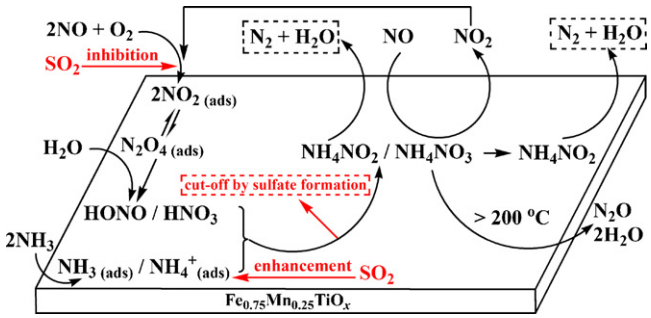

Scheme 1. Proposed mechanism of the NH_3-SCR reaction over Mn substituted iron titanate catalyst at low temperatures and the influence of SO_2 on the reaction pathway (as shown in red). (For interpretation of the references to color in this figure legend, the reader is referred to the web version of the article.)

to adsorbed NH_3 species (3361, 3257, 3159, 1676, 1603 and 1188 cm^{-1}) but also the bands ascribed to NH_4NO_3 species disappeared, with the remaining of nitrate species on the catalyst surface eventually. This result shows that the *in situ*-formed NH_4NO_3 was indeed reducible, thus being an important reactive intermediate species in the SCR reaction.

To further confirm the reactivity of NH_4NO_3 species, we also performed another *in situ* DRIFTS experiment in which NO + O_2 reacted with pre-impregnated NH_4NO_3 on the $Fe_{0.75}Mn_{0.25}TiO_x$ catalyst at 150 °C. During this process, we collected the spectrum of $Fe_{0.75}Mn_{0.25}TiO_x$ catalyst pre-impregnated with NH_4NO_3 and set as background, therefore the negative bands occurred in Fig. 7 indicated the surface species which were consumed in the reaction. As shown in the inserted figure, the bands nearly 1270 cm^{-1} firstly showed some increase in intensity after the introduction of NO + O_2 possibly due to the formation of partial extra NH_4NO_3 between NO_x and ionic NH_4^+, which were later overlapped by the strong negative bands from 1300 to 1500 cm^{-1}. These strong negative bands were caused by the reduction of pre-impregnated NH_4NO_3 by NO following the reaction equation of $NH_4NO_3 + NO \rightarrow NO_2 + N_2 + 2H_2O$ [29], which could also be confirmed by the N–H consumption bands at 3242, 3045 and 2835 cm^{-1} and the hydroxyl formation band at 3662 cm^{-1}. Because of different crystallization degrees of pre-impregnated NH_4NO_3 and *in situ*-formed surface NH_4NO_3, it was reasonable that the bands appeared in Fig. 7 showed some shift in position comparing with those in Figs. 2–6. Besides, the nitrate species including bridging nitrate (1614 or 1624 cm^{-1} and 1232 or 1219 cm^{-1}) and bidentate nitrate (1583 or 1585 cm^{-1}) also formed on the catalyst surface in this process. These results further confirmed that NH_4NO_3 was reducible by NO on the $Fe_{0.75}Mn_{0.25}TiO_x$ catalyst, playing the role as important reactive intermediate species in the SCR reaction at temperatures below 200 °C.

3.1.6. Proposed NH_3-SCR mechanism

Based on the *in situ* DRIFTS results in Sections 3.1.1–3.1.5, the NH_3-SCR mechanism over Mn substituted iron titanate catalyst at low temperatures is proposed and presented in Scheme 1. As shown in our previous study [20], the substitution of partial Fe by Mn in iron titanate catalyst greatly enhanced its NO oxidation ability at low temperatures. The *in situ*-produced NO_2 could strongly adsorb on the surface of $Fe_{0.75}Mn_{0.25}TiO_x$ catalyst, and then come through dimerization and disproportion into HONO and HNO_3 in the presence of H_2O. In the SCR reaction condition, NH_3 could strongly adsorb on the surface of catalyst as ionic NH_4^+ and coordinated NH_3, reacting with HONO and HNO_3 to form NH_4NO_2 and NH_4NO_3, respectively. Below 200 °C, NH_4NO_2 was very easy to decompose into N_2 and H_2O, while NH_4NO_3 could react with NO to produce NO_2 and NH_4NO_2 simultaneously [29,30]. The produced NO_2 could participate into the SCR reaction in another cycle, and the produced NH_4NO_2 could decompose into N_2 and H_2O directly. Since the surface NH_4NO_3 species was obviously present on the catalyst during this process, the reduction of NH_4NO_3 by NO was possibly the rate-determining step of the SCR reaction. Above 200 °C, NH_4NO_3 could also decompose into N_2O and H_2O [31], resulting in the decrease of N_2 selectivity of the SCR reaction. This was another possible route of N_2O formation besides of the unselective oxidation of NH_3 at relatively high temperatures [32].

Recently, Klukowski *et al.* [33] proposed an SCR reaction mechanism on dual Fe^{3+} sites over their Fe/HBEA zeolite catalyst using DRIFTS, XANES, TPD and kinetic measurements, in which the adsorbed NH_2 after NH_3 dehydrogenation reacted with adsorbed NO to form N_2 and H_2O. However, no NH_2 species on the Fe^{3+} sites was resolved in their DRIFTS experiments. Therefore, we cannot exclude the possibility that adsorbed NH_3 species over our $Fe_{0.75}Mn_{0.25}TiO_x$ catalyst would undergo dehydrogenation by Fe^{3+} or Mn^{3+} to form NH_2 species and then react with adsorbed NO_x species to form N_2 and H_2O, although this reaction pathway might not be important in the low temperature range below 200 °C. Besides, Iwasaki *et al.* [31] and Grossale *et al.* [34] concluded that the high concentrations of NH_3 on the surface of Fe/ZSM-5 catalyst would inhibit its low temperature SCR activity, because of the inhibition of NO oxidation or the capture of reactive nitrate species by strongly adsorbed NH_3. Similar inhibition effect might also exist over our $Fe_{0.75}Mn_{0.25}TiO_x$ catalyst, although it was not investigated in this study. In our future study, we can optimize the SCR reaction atmosphere (such as the gas phase NH_3 concentration) or modify the acid–base property of the catalyst surface to lower the undesired inhibition effect of NH_3 [34], further improving its low temperature SCR activity.

3.2. H_2O/SO_2 inhibition effect on NH_3-SCR over $Fe_{0.75}Mn_{0.25}TiO_x$

3.2.1. Influence of H_2O/SO_2 on NO_x conversion in the NH_3-SCR reaction

For practical use of this Mn substituted iron titanate catalyst, the influence of H_2O and SO_2 on the SCR activity needs to be investigated. As the results shown in Fig. 8, when 10 vol.% H_2O was added into the flue gas, a sharp decline of the NO_x conversion (to *ca.* 70%) was firstly observed, which then partially recovered and maintained at 90% for the next 48 h; after the removal of H_2O, the NO_x conversion recovered to the original level rapidly, indicating that the inhibition effect of H_2O on the SCR activity over $Fe_{0.75}Mn_{0.25}TiO_x$ catalyst was mild and reversible. On the con-

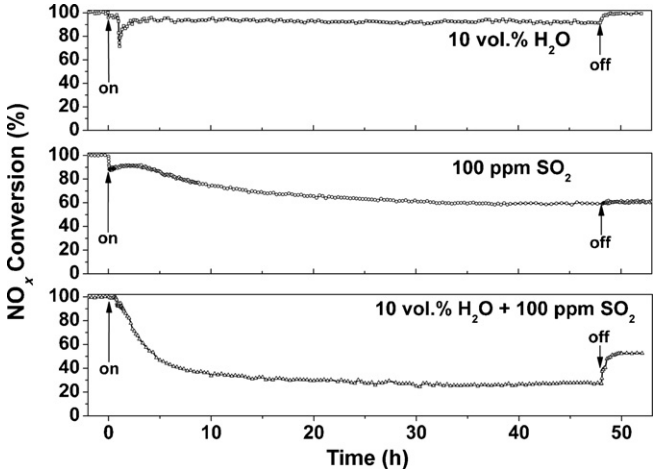

Fig. 8. Influence of H_2O/SO_2 on NO_x conversion in the NH_3-SCR reaction on the $Fe_{0.75}Mn_{0.25}TiO_x$ catalyst at 250 °C.

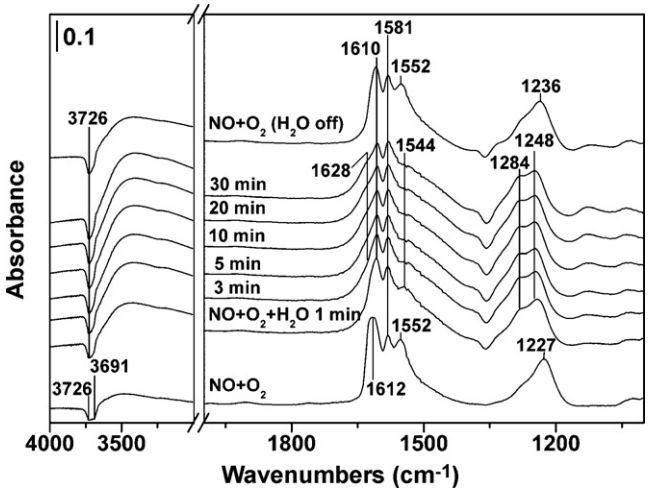

Fig. 10. *In situ* DRIFTS of the influence of H_2O on $NO + O_2$ adsorption on the $Fe_{0.75}Mn_{0.25}TiO_x$ catalyst at 150 °C.

trary, the inhibition effect of SO_2 was much more intense and irreversible: only *ca.* 60% NO_x conversion was obtained in the presence of 100 ppm SO_2 for 48 h test and no recover was observed after the removal of SO_2. The coexistence of H_2O and SO_2 led to more serious activity decline, yet no synergistic inhibition effect was observed; only the activity loss caused by H_2O was recovered after stopping $H_2O + SO_2$, implying again that the SO_2 poisoning was irreversible. On the one hand, the Mn substitution could obviously enhance the SCR activity of $Fe_{0.75}Mn_{0.25}TiO_x$ catalyst at low temperatures, yet on the other hand it also resulted in the decrease of SO_2 resistance. This catalyst should be used in SO_2-free atmosphere, such as flue gas after desulfurization and dust removal. The H_2O/SO_2 inhibition mechanism will be clarified in the following sections using *in situ* DRIFTS methods.

3.2.2. Influence of H_2O on NH_3/NO_x adsorption

As we mentioned above, both NH_3 and NO_x adsorbed species existed on the catalyst surface participating into the SCR reaction, therefore the influence of H_2O on NH_3/NO_x adsorption was firstly investigated. As shown in Fig. 9, after the introduction of H_2O, the bands at 1680 and 1448 cm^{-1} attributed to ionic NH_4^+ showed some increase in intensity due to the hydroxylation of catalyst surface in the presence of H_2O. At the same time, the bands at 1603 and 1178 cm^{-1} (with some blue shift to 1192 cm^{-1}) attributed to coordinated NH_3 showed some decrease in intensity, mainly due to the transformation of partial Lewis acid sites into Brønsted acid sites in the hydroxylation process. The band at 1632 cm^{-1} (δ_{HOH} vibration mode) [35,36] was ascribed to the adsorption of H_2O on the surface of catalyst, which totally disappeared after the removal of H_2O feed. The hydroxylation effect was also vanished after stopping the H_2O supply, accompanied by the simultaneous decrease of ionic NH_4^+ bands and increase of coordinated NH_3 bands in intensity.

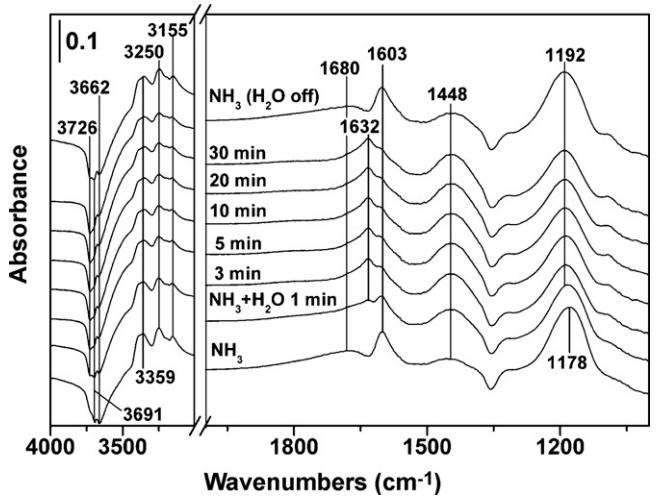

Fig. 9. *In situ* DRIFTS of the influence of H_2O on NH_3 adsorption on the $Fe_{0.75}Mn_{0.25}TiO_x$ catalyst at 150 °C.

Fig. 10 shows the *in situ* DRIFTS spectra of influence of H_2O on NO_x adsorption on the $Fe_{0.75}Mn_{0.25}TiO_x$ catalyst at 150 °C. After the introduction of H_2O, both bridging nitrate (1612 and 1227 cm^{-1}) and monodentate nitrate (1552 cm^{-1}) showed some decrease in intensity, while bidentate nitrate (1581 cm^{-1}) showed no obvious change during the whole process. Due to the adsorption and disturbance of H_2O on the surface of catalyst (shoulder band at 1628 cm^{-1} for δ_{HOH} vibration mode), the ν_3 low vibration mode of bridging nitrate showed some blue shift to 1248 cm^{-1} due to the reduction of splitting of ν_3 frequency [37]; the ν_3 low vibration mode of monodentate nitrate also appeared at 1284 cm^{-1} [36]. After the removal of H_2O feed, the surface nitrate species recovered to the original level, similar as adsorbed NH_3 species. Summarizing the results in Figs. 9 and 10 we can conclude that, the inhibition effect of H_2O on the adsorption of NH_3 and NO_x on the $Fe_{0.75}Mn_{0.25}TiO_x$ catalyst was mild and reversible, which is in well accordance with the SCR activity results in Fig. 8; the slight activity decline in the presence of H_2O was mainly caused by the competitive adsorption of H_2O with partial reactive bridging nitrate and monodentate nitrate.

3.2.3. Influence of SO_2 on NH_3/NO_x adsorption

Comparatively, the influence of SO_2 on NH_3/NO_x adsorption on the $Fe_{0.75}Mn_{0.25}TiO_x$ catalyst was also investigated at 150 °C. As the results shown in Fig. 11, after the introduction of $SO_2 + O_2$, the bands at 1684 and 1437 cm^{-1} attributed to ionic NH_4^+ showed strong increase in intensity due to the sulfation of catalyst surface and simultaneous enhancement of surface acidity. The bands at 1603 and 1182 cm^{-1} ascribed to coordinated NH_3 showed some decrease in intensity, and the latter one was even overlapped by the growing bands attributed to sulfate species (1240, 1159 and 1051 cm^{-1} for ν_3 band splitting of SO_4^{2-}) [38]. In the N–H stretching vibration region, the bands also shifted from 3359, 3251 and 3153 cm^{-1} of coordinated NH_3 to 3209, 3049 and 2835 cm^{-1} of ionic NH_4^+ [21], indicating the formation of a large amount of extra Brønsted acid sites during the sulfation process. The strongly

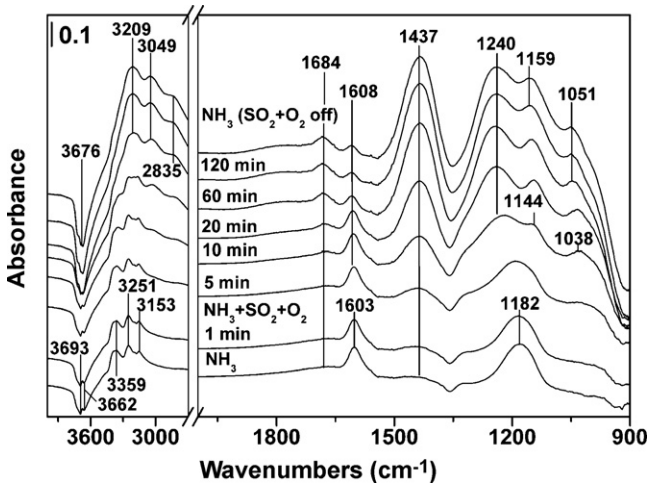

Fig. 11. *In situ* DRIFTS of the influence of SO_2 on NH_3 adsorption on the $Fe_{0.75}Mn_{0.25}TiO_x$ catalyst at 150 °C.

adsorbed NH_4^+ species on these Brønsted acid sites introduced by sulfate species inhibited the further adsorption of reactive coordinated NH_3 on Lewis acid sites, which probably resulted in the decrease of SCR activity to a certain extent. After the removal of $SO_2 + O_2$, the adsorbed surface species showed no obvious change.

Fig. 12 shows the *in situ* DRIFTS spectra of influence of SO_2 on NO_x adsorption on the $Fe_{0.75}Mn_{0.25}TiO_x$ catalyst at 150 °C. After the introduction of SO_2 into the $NO + O_2$ feeding gas, the surface nitrate species at 1614, 1581, 1554 and 1228 cm^{-1} quickly disappeared with the increasing of time, replaced by the deposited sulfate species (1363 and 1282 cm^{-1} for $\nu_{asS=O}$ and $\nu_{sS=O}$, 1200, 1144 and 1038 cm^{-1} for ν_3 band splits) [38–40] and adsorbed H_2O (δ_{HOH} vibration mode) formed in the sulfation process. After the removal of SO_2 from the feeding gas, the nitrate species did not recover at all, suggesting that the inhibition effect of SO_2 on NO_x adsorption on the $Fe_{0.75}Mn_{0.25}TiO_x$ catalyst was intense and irreversible. Summarizing the results in Figs. 11 and 12 we can conclude that, although the NH_3 adsorption was greatly enhanced in the presence of SO_2, the formation of surface nitrate species was intensely and irreversibly inhibited by the formation of sulfate species, resulting in the cut-off of the SCR reaction pathway that we proposed in Scheme 1 (as shown in red). This is in well accordance with the SCR activity results in Fig. 8, in which the activity decline

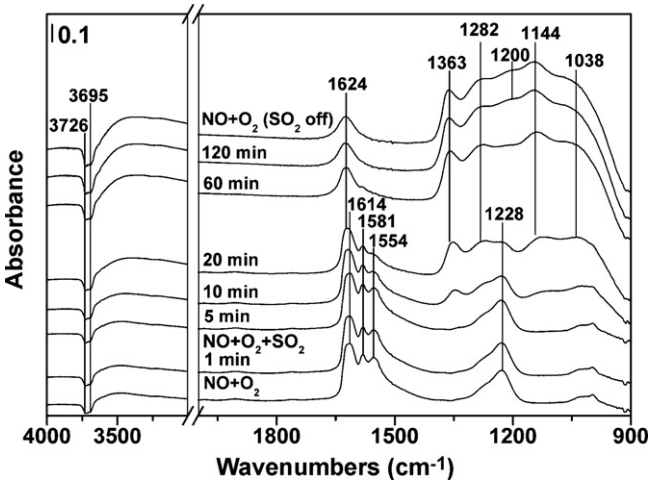

Fig. 12. *In situ* DRIFTS of the influence of SO_2 on $NO + O_2$ adsorption on the $Fe_{0.75}Mn_{0.25}TiO_x$ catalyst at 150 °C.

caused by SO_2 poisoning could not recover after the removal of SO_2 or $H_2O + SO_2$.

4. Conclusions

The NH_3-SCR reaction mechanism over Mn substituted iron titanate catalyst was fully investigated using *in situ* DRIFTS methods. On the $Fe_{0.75}Mn_{0.25}TiO_x$ catalyst at low temperatures, both ionic NH_4^+ and coordinated NH_3 contributed to the SCR reaction; bridging nitrate and monodentate nitrate were confirmed to be the reactive nitrate species. In the real SCR reaction condition, surface NH_4NO_3 was formed, playing the role as an important intermediate species. The reactivity of NH_4NO_3 was also proved, and the reduction of NH_4NO_3 by NO was possibly the rate-determining step of the whole SCR reaction. At temperatures above 200 °C, the decomposition of NH_4NO_3 might be another source of N_2O formation besides of the unselective oxidation of NH_3. The inhibition effect of H_2O on the SCR activity was mild and reversible, because only slight and reversible inhibition of NH_3/NO_x adsorption by H_2O was observed. On the contrary, the inhibition effect of SO_2 was much more intense and irreversible, because the nitrate formation was totally inhibited by the deposition of sulfate species, resulting in the cut-off of the SCR reaction pathway that we proposed.

Acknowledgements

This work was financially supported by the Chinese Academy of Sciences (KZCX1-YW-06-04) and the National High Technology Research and Development Program of China (2009AA064802 and 2009AA06Z301).

Appendix A. Supplementary data

Supplementary data associated with this article can be found, in the online version, at doi:10.1016/j.cattod.2010.02.043.

References

[1] H. Bosch, F. Janssen, Catal. Today 2 (1988) 369.
[2] Z. Zhu, Z. Liu, S. Liu, H. Niu, Appl. Catal. B: Environ. 30 (2001) 267.
[3] A. Boyano, M.J. Lázaro, C. Cristiani, F.J. Maldonado-Hodar, P. Forzatti, R. Moliner, Chem. Eng. J. 149 (2009) 173.
[4] T. Valdés-Solís, G. Marbán, A.B. Fuertes, Appl. Catal. B: Environ. 46 (2003) 261.
[5] G. Qi, R.T. Yang, Appl. Catal. B: Environ. 44 (2003) 217.
[6] G. Qi, R.T. Yang, R. Chang, Catal. Lett. 87 (2003) 67.
[7] J. Huang, Z. Tong, Y. Huang, J. Zhang, Appl. Catal. B: Environ. 78 (2008) 309.
[8] F. Kapteijn, L. Singoredjo, A. Andreini, J.A. Moulijn, Appl. Catal. B: Environ. 3 (1994) 173.
[9] M. Kang, T.H. Yeon, E.D. Park, J.E. Yie, J.M. Kim, Catal. Lett. 106 (2006) 77.
[10] X. Tang, J. Hao, W. Xu, J. Li, Catal. Commun. 8 (2007) 329.
[11] P.R. Ettireddy, N. Ettireddy, S. Mamedov, P. Boolchand, P.G. Smirniotis, Appl. Catal. B: Environ. 76 (2007) 123.
[12] P.G. Smirniotis, P.M. Sreekanth, D.A. Peña, R.G. Jenkins, Ind. Eng. Chem. Res. 45 (2006) 6436.
[13] T. Grzybek, J. Pasel, H. Papp, Phys. Chem. Chem. Phys. 1 (1999) 341.
[14] M. Kang, E.D. Park, J.M. Kim, J.E. Yie, Catal. Today 111 (2006) 236.
[15] G. Qi, R.T. Yang, R. Chang, Appl. Catal. B: Environ. 51 (2004) 93.
[16] F. Eigenmann, M. Maciejewski, A. Baiker, Appl. Catal. B: Environ. 62 (2006) 311.
[17] F. Liu, H. He, C. Zhang, Chem. Commun. (2008) 2043.
[18] F. Liu, H. He, C. Zhang, Z. Feng, L. Zheng, Y. Xie, T. Hu, Appl. Catal. B: Environ. (2010), doi:10.1016/j.apcatb.2010.02.038.
[19] F. Liu, H. He, C. Zhang, Environ. Sci. Technol., submitted for publication.
[20] F. Liu, H. He, Y. Ding, C. Zhang, Appl. Catal. B: Environ. 93 (2009) 194.
[21] N.Y. Topsøe, Science 265 (1994) 1217.
[22] G. Ramis, L. Yi, G. Busca, Catal. Today 28 (1996) 373.
[23] R.Q. Long, R.T. Yang, J. Catal. 186 (1999) 254.
[24] G.M. Underwood, T.M. Miller, V.H. Grassian, J. Phys. Chem. A 103 (1999) 6184.
[25] W.S. Kijlstra, D.S. Brands, E.K. Poels, A. Bliek, J. Catal. 171 (1997) 208.
[26] W.S. Kijlstra, D.S. Brands, H.I. Smit, E.K. Poels, A. Bliek, J. Catal. 171 (1997) 219.
[27] G. Madia, M. Koebel, M. Elsener, A. Wokaun, Ind. Eng. Chem. Res. 41 (2002) 4008.
[28] G. Piazzesi, M. Elsener, O. Kröcher, A. Wokaun, Appl. Catal. B: Environ. 65 (2006) 169.

[29] A. Grossale, I. Nova, E. Tronconi, D. Chatterjee, M. Weibel, J. Catal. 256 (2008) 312.
[30] A. Savara, M.J. Li, W.M.H. Sachtler, E. Weitz, Appl. Catal. B: Environ. 81 (2008) 251.
[31] M. Iwasaki, K. Yamazaki, H. Shinjoh, Appl. Catal. A: Gen. 366 (2009) 84.
[32] G. Busca, L. Lietti, G. Ramis, F. Berti, Appl. Catal. B: Environ. 18 (1998) 1.
[33] D. Klukowski, P. Balle, B. Geiger, S. Wagloehner, S. Kureti, B. Kimmerle, A. Baiker, J.-D. Grunwaldt, Appl. Catal. B: Environ. 93 (2009) 185.
[34] A. Grossale, I. Nova, E. Tronconi, J. Catal. 265 (2009) 141.
[35] R.C. Adams, L. Xu, K. Moller, T. Bein, W.N. Delgass, Catal. Today 33 (1997) 263.
[36] A.L. Goodman, E.T. Bernard, V.H. Grassian, J. Phys. Chem. A 105 (2001) 6443.
[37] Y. Ji, T.J. Toops, U.M. Graham, G. Jacobs, M. Crocker, Catal. Lett. 110 (2006) 29.
[38] H. Fu, X. Wang, H. Wu, Y. Yin, J. Chen, J. Phys. Chem. C 111 (2007) 6077.
[39] H. Watanabe, C.D. Gutleben, J. Seto, Solid State Ionics 69 (1994) 29.
[40] D. Pietrogiacomi, A. Magliano, D. Sannino, M.C. Campa, P. Ciambelli, V. Indovina, Appl. Catal. B: Environ. 60 (2005) 83.